TWENTY-FIRST CENTURY LEVEE OVERTOPPING PROJECTIONS FROM InSAR-DERIVED SUBSIDENCE RATES IN THE SACRAMENTO-SAN JOAQUIN DELTA, CALIFORNIA: 2006–2010

A White Paper from the California Energy Commission's California Climate Change Center

Prepared for: California Energy Commission

Prepared by: School of Ocean and Earth Science and Technology, University of Hawaii

JULY 2012

CEC-500-2012-018

Benjamin A. Brooks
Deepak Manjunath

School of Ocean and Earth Science and Technology
University of Hawaii, Honolulu, HI

ACKNOWLEDGEMENTS

This work was funded by the Public Interest Energy Research (PIER) program of the California Energy Commission, grant 500-09-035 to the School of Ocean and Earth Sciences and Technology at the University of Hawaii: Contemporaneous Subsidence and Levee Overtopping Vulnerability, Sacramento-San Joaquin Delta, California. We gratefully acknowledge Dan Cayan at Scripps Institute of Oceanography and Noah Knowles at the United States Geological Survey, for discussion and suggestions.

ABSTRACT

To provide an updated synoptic assessment of vertical land motion rates in the Sacramento-San Joaquin Delta, the research team performed synthetic aperture radar interferometry (InSAR) on 35 radar scenes from the Envisat platform acquired from 2006–2010. The study used contemporaneously collected continuous global positioning system data to tie the InSAR results to an absolute reference frame. In accord with the researchers' previous study from 1995–2000 (VLM00), the new results (VLM10) demonstrate general subsidence of the Delta with respect to its margins. The average rates of ~1-2 millimeters per year (mm/yr) are slightly lower than the ~3-5mm/yr rates from 1995–2000. An unexpected finding is the uplift associated with Roberts Island, in the Delta's southeastern sector. The time- and space-varying differences between the two solutions (VLM00 and VLM10) highlights the need to develop a physical model for the Delta. The study used the updated ground-motion rate map and the most current twenty-first century sea-level rise predictions to project when Delta levees will subside below high-water design thresholds. The study showed that the time period between 2050–2075 is a critical time period, when levees will start to fall below design thresholds, and by 2100 most Delta levees will probably do so.

Keywords: subsidence, Synthetic Aperture Radar Interferometry (InSAR), levees, overtopping, peat

Please use the following citation for this paper:

Brooks, Benjamin A., and Deepak Manjunath (School of Ocean and Earth Sciences and Technology, University of Hawaii). 2012. ***Twenty-First Century Levee Overtopping Projections from InSAR-Derived Subsidence Rates in the Sacramento-San Joaquin Delta, California: 2006–2010.*** California Energy Commission. Publication number: CEC-500-2012-018.

TABLE OF CONTENTS

LIST OF FIGURES

LIST OF TABLES

Unless otherwise noted, all tables and figures are provided by the author.

EXECUTIVE SUMMARY

Introduction

The Sacramento-San Joaquin Delta helps provide fresh water to about 1 million cultivated hectares and more than two-thirds of California's human population. The Delta's islands help maintain fresh-water quality in California by acting as a barrier to seasonally and tidally driven saline incursions from the San Francisco Bay. Land subsidence, however, thought to occur primarily by oxidation of surface peat soils drained for agricultural purposes, has left island elevations as much as ~8 meters (m) below sea-level. The islands are protected by a system of earthen levees. In the event of a levee failure, rapid island-infilling can draw brackish water back into the Delta and seriously degrade fresh-water quality and supply throughout the State of California. Failure can occur due to a number of forcings, including seismic shaking, elevated hydraulic head, and high-water overtopping.

Susceptibility to high-water overtopping is directly related to rates of vertical land motion of the levees themselves combined with sea-level change rates. Classical methods for studying vertical land motion, such as leveling, are too labor- and time-intensive to perform in a comprehensive way throughout the Delta. The authors showed previously that using satellite-based synthetic aperture radar interferometry (InSAR) it is possible to design and implement a Delta-wide strategy to monitor synoptically vertical land motion of Delta levees. Those studies found that the Delta levee system was subsiding at rates of 3–5 millimeters per year (mm/yr), and that when combined with sea-level rise scenarios it was probable that the design thresholds of levees would be exceeded and widespread.

Purpose

The purposes of this project were:

- To confirm and update the previous InSAR-derived vertical land motion findings for the Delta using newly available data from 2006–2010.
- To combine the vertical land motion results with updated global sea-level rise scenarios to create the most accurate and up-to-date twenty-first century levee overtopping projections for the Delta

Objectives

The principal objectives of this project were:

- To perform synthetic aperture radar interferometry on 35 radar scenes from the Envisat platform acquired from 2006–2010.
- To use contemporaneously collected continuous global positioning system (GPS) data to tie the InSAR results to an absolute reference frame.
- To compare the most current results with similar results from 1995–2000, to both confirm the validity of the earlier results and to document any time- or space-variation in vertical land motion rates.
- To use the most current sea-level rise projections and the most current subsidence rates, to project when Delta levees will subside below high-water design thresholds.

Conclusions and Recommendations

The study resulted in the following conclusions:

- From 2006–2010 the Delta subsided with respect to its margins.
- The general subsidence pattern replicates our previous results from 1995–2000 but at rates of 1–2 mm/yr versus 3–5 mm/yr.
- An unexpected finding is the moderate uplift associated with Roberts Island in the Delta's southeastern sector.
- If future Delta-wide subsidence patterns and rates follow the presently observed ones, and sea-level rise rates follow the most currently accepted projections, then between 2035–2050 levees are expected to start subsiding below high-water design thresholds. By 2065–2075 at least 90 percent of the levees are likely to have subsided below high-water design thresholds.

The study team offers the following recommendations:

- The changes in rates between 1995–2000 and 2006–2010, as well as the spatially varying pattern of vertical land motion evidenced by uplift at Roberts Island, motivates the need for a comprehensive stratigraphic and hydrological model of the Delta that takes into account the InSAR-determined rates.
- The acquisition and processing of InSAR data should be part of a future levee subsidence monitoring strategy that iteratively updates projections as new data and/or sea-level rise projections become available.

1.0 Introduction

The Sacramento-San Joaquin Delta provides fresh water to ~1 million cultivated hectares and more than two-thirds of California's human population (Figure 1) (Lund et al. 2007). More than 60 Delta islands, particularly the four westernmost, help maintain the fresh-water quality by acting as barriers to seasonally and tidally driven saline incursions from the San Francisco Bay (Galloway et al. 1999; Lund et al. 2010). Land subsidence since the late 1800s, thought to occur primarily by oxidation of peat soils drained for agricultural purposes (Deverel and Rojstaczer 1996; Deverel and Leighton 2010; Deverel et al. 1998; Mount and Twiss 2005; Rojstaczer and Deverel 1993; 1995; Rojstaczer et al. 1991) has left many Delta island elevations as much as ~8 meters (m) below sea-level (Coons et al. 2008) (Figure 1). The islands are protected by more than 1700 kilometers (km) of earthen levees whose structural stability is variable (over 100 levee failures have occurred since the 1890s) and poorly known (Mount and Twiss 2005; Suddeth et al. 2010). In the event of a levee failure, rapid island-infilling can draw brackish water back into the Delta and seriously degrade fresh-water quality and supply.

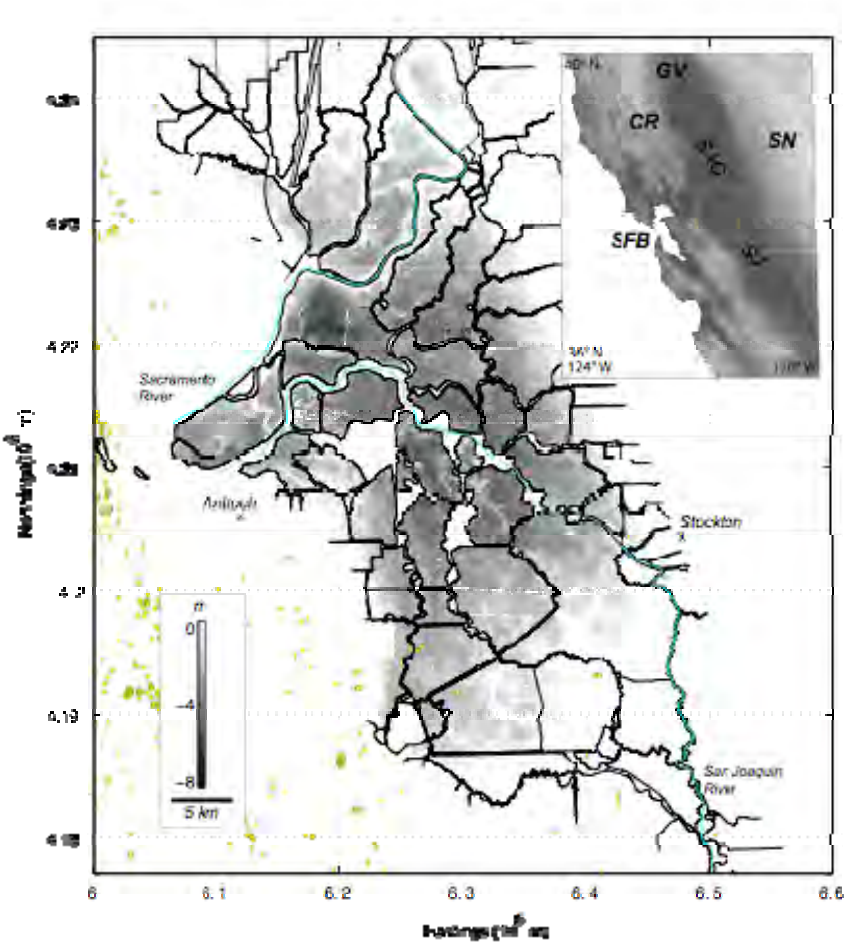

Figure 1. (Inset) Topographic Map of Central-Northern California. SFB, San Francisco Bay; SN, Sierra Nevada Mountains; CR, Coast Range Mountains; SAC, Sacramento River Valley; SJ, San Joaquin River Valley. Yellow box, study region. (Body) Grey-scale topography of the Delta region from Coons et al. (2008), only showing values less than 0 m. Heavy black lines, levee locations.

Although the structural resistance to seismic-shaking and local differential land subsidence is most often the principal factor considered when determining levee vulnerability, susceptibility to high water overtopping exacerbated by subsidence (one of the principal levee failure modes during Hurricane Katrina in 2005 [Dixon et al. 2006]) is also a significant threat (DWR 2009) especially in the context of accelerating twenty-first century global sea-level rise (SLR) projections (Vermeer and Rahmstorf 2009). In the Delta, local geodetic studies demonstrate that some islands have subsided at rates of ~4–70 millimeters per year (mm/yr) during the past century and that island interiors have subsided by greater amounts than their margins (Deverel and Rojstaczer 1996; Deverel and Leighton 2010; Deverel et al. 1998; Mount and Twiss 2005). Given that measured subsidence rates in the Delta (Brooks et al. in press; Deverel and Rojstaczer 1996; Deverel and Leighton 2010; Deverel et al. 1998; Rojstaczer and Deverel 1995) are of the same order of magnitude, or up to 70 times the currently observed rate of global SLR (~1–3 mm/yr) (Church and White 2006; Woppelmann et al. 2009), quantifying Delta-wide subsidence is essential to best inform mitigation and planning decisions attempting to balance ecosystem health and anthropogenic needs.

Our recent work showed that satellite-based InSAR (interferometric synthetic aperture radar) is an effective remote-sensing tool that provides unprecedented ability to monitor synoptically Delta-wide vertical land motion (VLM) rates (Brooks et al. in press). We found a broad-based pattern of downward VLM within the Delta. Over most of the region these subsidence rates ranged from 5 to 20 mm/yr (Figure 2). Superimposed on this overall downward motion were seasonal changes associated with the wetting and drying of the Delta (the seasonal changes were also not correlated with hydrocarbon extraction-related activities). In contrast to the previous commonly accepted understanding, however, our analysis suggested that, because the measurements are not correlated with peat thickness variations over Delta-island length scales, and because they are significantly lower than the locally measured peat-related subsidence rates, it is most likely that the InSAR rates do not reflect Delta island peat compaction. Rather, we suggested that the InSAR-derived rates reflected the ongoing, slower compaction of the Delta's underlying Holocene mineral soils and sedimentary column.

The synoptic nature of the measurements and the myriad returns from the levees also allowed us to couple the InSAR measurements with SLR projections and to provide a matrix of Delta-wide levee overtopping potential for the twenty-first century. We found that between 2050 and 2100 there was a high probability that a large (> 50 percent) portion of the Delta levees would have subsided below the Public Law 84-99 standard wherein levees are designed to have ~0.5 m (1.5 ft.) freeboard above the 100-year flood stage (Betchart 2008) (Figure 3).

The purpose of this current contribution is to provide more accurate twenty-first century projections using InSAR-derived subsidence rates over the Delta for the most current time period (the initial InSAR rates were measured from 1995–2000) and more recent SLR projections.

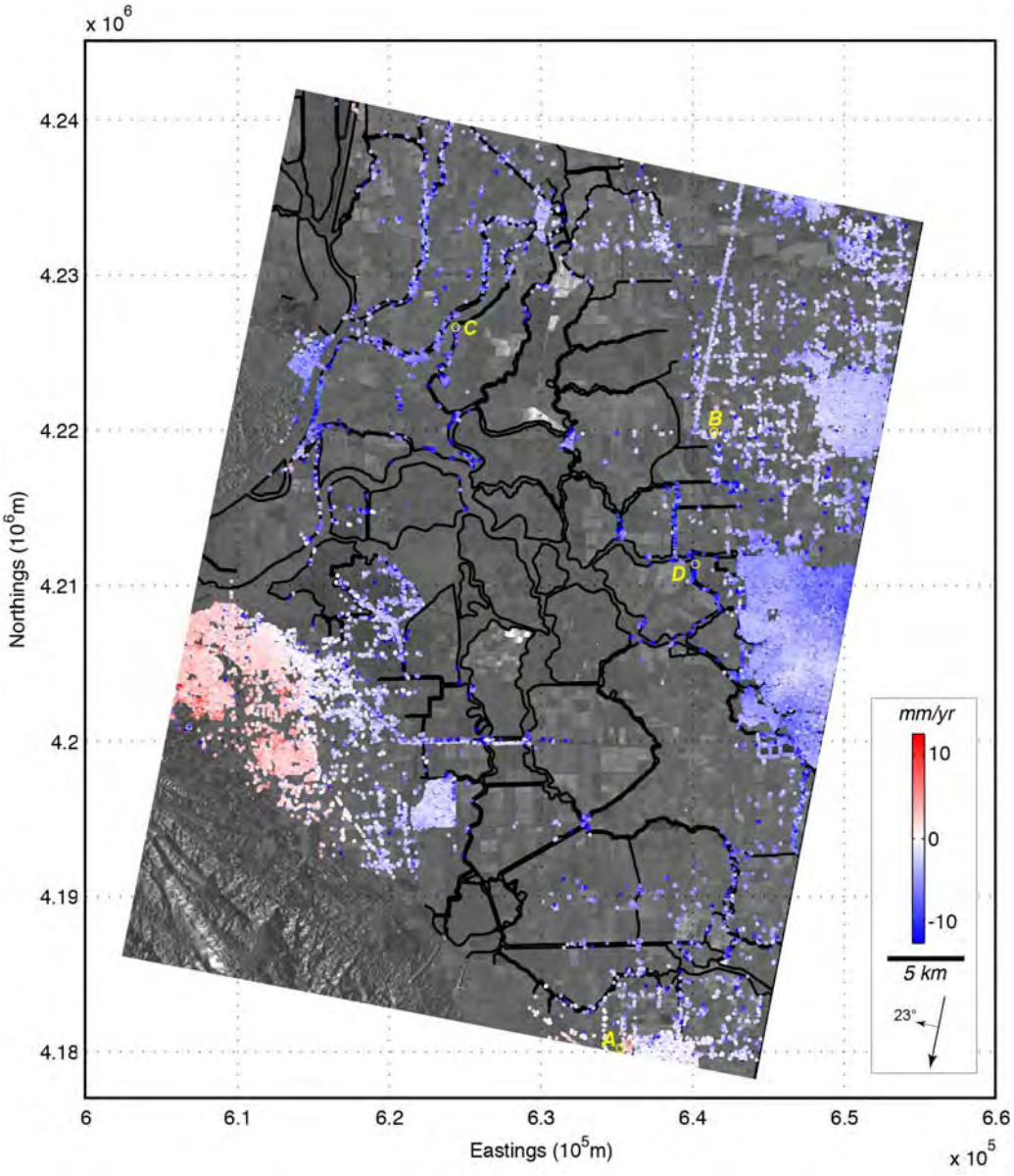

Source: Brooks et al. in press

Figure 2. Annual Vertical Displacement Rates (Colored Circles) for All Scatterers from the 1995–2000 Data Set

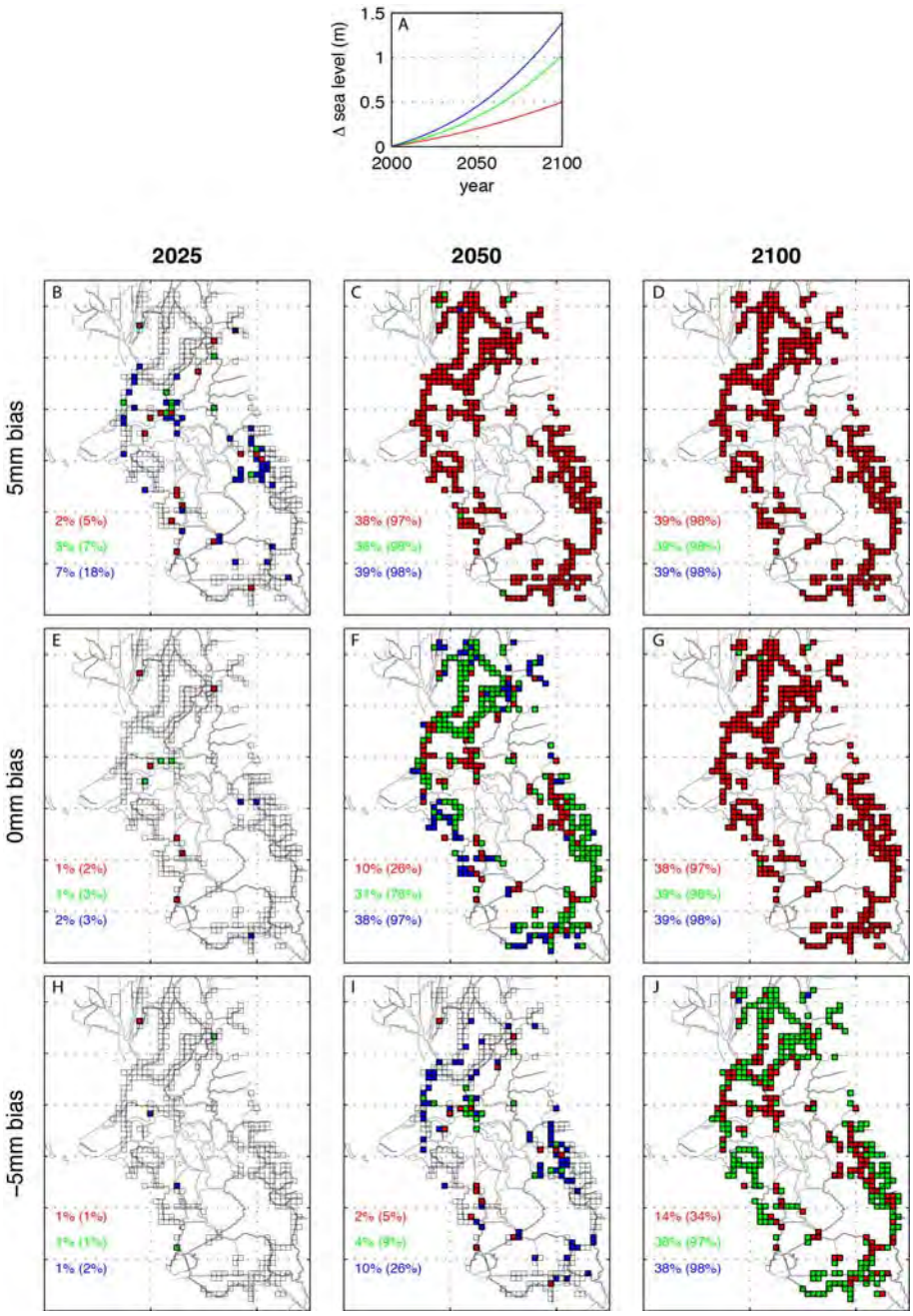

Source: Brooks et al. (in press)

Figure 3. (A) Projected Sea-level Rise in the Delta for Low (red), Medium (green), and High (blue) Scenarios. (B-J) Projected areas below 0.5 m of current elevation for 21st-century dates (columns), potential reference frame biases (rows), and sea-level rise scenarios (colored as in A). Colored text indicates percentage below threshold level: no parentheses indicates all levees with InSAR measurements; parentheses indicates all levees.

2.0 Methods

2.1 Synthetic Aperture Radar Interferometry (InSAR)

Space-based synthetic aperture radar interferometry (InSAR) (Burgmann et al. 2000) was used to measure synoptically Delta ground-motion with sub-centimeter motion resolution from 35 descending Envisat scenes acquired along Descending Track 70 and Frame 2835 (Table 1). The temporal coverage of the data sets ranged from February 2006 through February 2010. Orbit 32689 was used as the reference scene (Master), relative to which 35 interferograms were computed.

Table 1. List of Envisat Scenes Used for InSAR Processing. The italicized entry is the master scene with respect to which all other scenes are referenced.

	Orbit #	Acquisition Date
1	20665	2006 2 11
2	21166	2006 3 18
3	21667	2006 4 22
4	22168	2006 5 27
5	22669	2006 7 1
6	23170	2006 8 5
7	24172	2006 10 14
8	24673	2006 11 18
9	25174	2006 12 23
10	28180	2007 7 21
11	28681	2007 8 25
12	29182	2007 9 29
13	29683	2007 11 3
14	30184	2007 12 8
15	30685	2008 1 12
16	31186	2008 2 16
17	31687	2008 3 22
18	32188	2008 4 26
19	***32689***	***2008 5 31***
20	33190	2008 7 5
21	33691	2008 8 9
22	34192	2008 9 13
23	35194	2008 11 22
24	36196	2009 1 31
25	36697	2009 3 7
26	37198	2009 4 11
27	37699	2009 5 16
28	38200	2009 6 20
29	38701	2009 7 25
30	39202	2009 8 29
31	39703	2009 10 3
32	40204	2009 11 7
33	40705	2009 12 12
34	41206	2010 1 16
35	41707	2010 2 20

Our general processing approach is identical to that described in detail previously (Brooks et al., in press) and so only a brief summary is given here. Traditional InSAR performance is compromised when interferometric coherence is degraded, due to either phase instability of specific portions of the reflective surface or satellite orbital baselines exceeding a critical distance threshold. Here, to increase temporal and spatial resolution due to poor interferometric coherence in the highly cultivated Delta, we employ the recently developed "persistent scatterer" interferometry (PSInSAR) technique (Ferretti et al. 2001; Hooper et al. 2004). PSInSAR utilizes the fact that minimal baseline-related decorrelation occurs for stable, point-like reflectors, and so the interferometric phase may be interpreted even for scene pairs with long perpendicular baselines that may exceed the critical baseline. For a general discussion of the PSInSAR technique, see Kampes (2006). We employ the technique of Werner (Brooks et al. 2007; Werner et al. 2003) and determine point targets using joint measures of backscatter temporal amplitude variability and spatial spectral diversity of candidate points (Ferretti et al. 2001).

2.2 Continuous GPS (CGPS)

Continuous global positioning system (CGPS) measurements were used, both as ground-truth of the InSAR-determined rates, and also because InSAR alone provides only a relative measure of ground motion, to provide a tie to a global, GPS-defined reference frame. Within the footprint of the Envisat scenes (Figure 1) there are three CGPS stations from the Plate Boundary Observatory (PBO).[1] In contrast to our previous study, these stations (P274, P273, and P256) were all in operation since early 2006, so they can be used to provide a true contemporaneous reference frame tie for the InSAR data set.

The Plate Boundary Observatory CGPS stations are all high-stability deep-drilled, braced monuments[2] with leg depths of ~12 meters. Plate Boundary Observatory CGPS displacement time series are calculated by merging daily position time series solutions determined by two different analysis centers (New Mexico Institute of Mining and Technology and Central Washington University) with independent processing packages (GAMIT and Gipsy, respectively) and satellite orbital solutions.[3] The Analysis Center Coordinator (Massachusetts Institute of Technology) takes the two solutions, rotates them into a common reference frame, merges them, and aligns the combined solution to the ITRF 2008 global Reference Frame,[4] which is an update of the ITRF 2005 frame and uses the same processing strategy (Altamimi et al. 2007).

Velocities are estimated by identifying and removing a seasonal sinusoid and then linearly regressing the residual velocity (Figure 4). This is a particularly effective strategy given that: (a) the time series appear to be well-described by a model combining seasonal motion with a linear rate and, (b) each series has an approximately four-year time span that allows for clear identification of the seasonal signal (Figure 4).

---

[1] See UNAVCO, Plate Boundary Observatory at http://pboweb.unavco.org/

[2] UNAVCO, Permanent Station GPS/GNSS http://facility.unavco.org/project_support/permanent/monumentation/deepdrilled.html.

[3] http://pbo.unavco.org/news/highlight/77

[4] ITRF2008. http://itrf.ensg.ign.fr/ITRF_solutions/2008/.

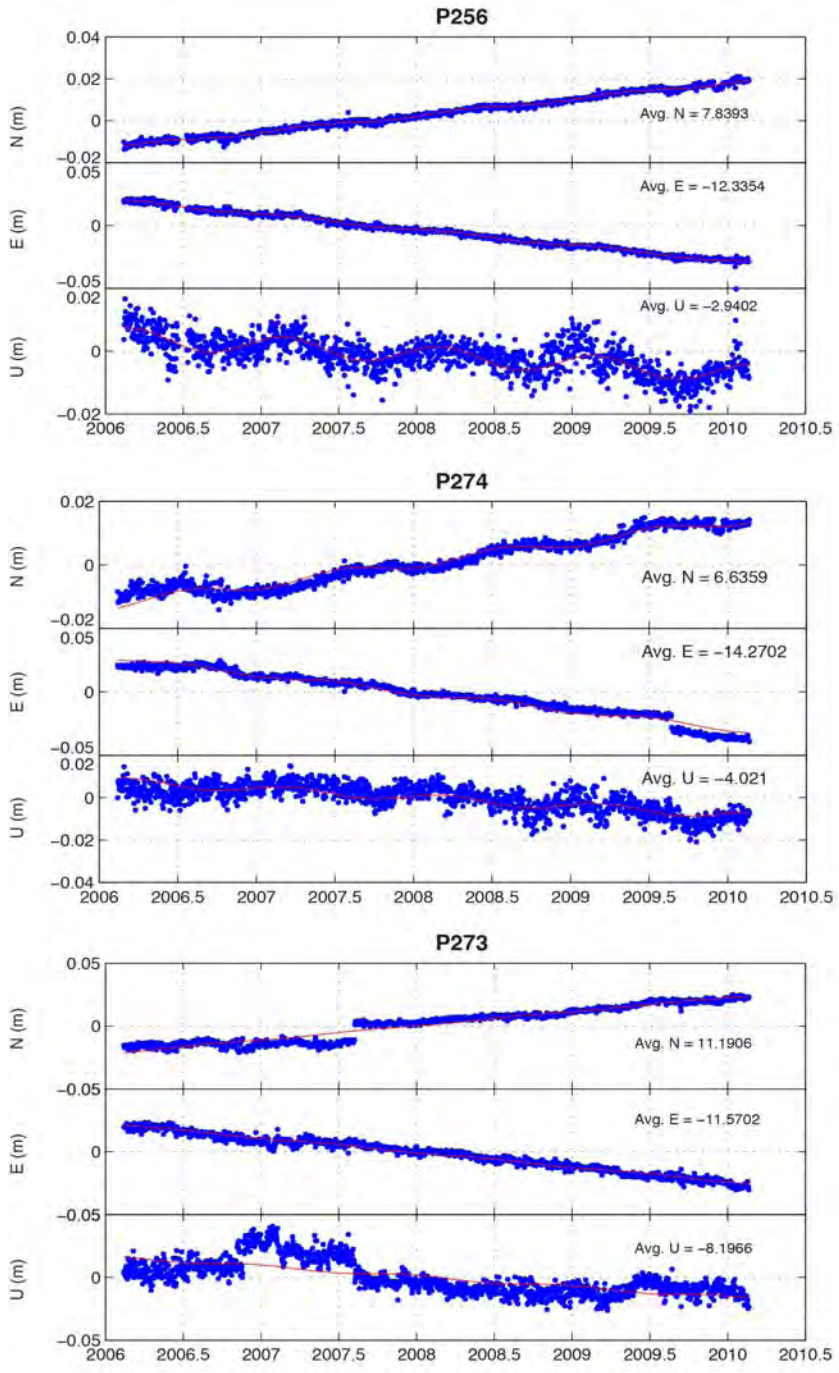

Figure 4. Continuous GPS Daily Solutions for Three Sites in the Delta, Locations on Figure 5. N, north component; E, east component; U, up component.

Additionally, an offset is identified and removed in the time series for site P273 on August 8, 2007. The offset is removed in our analysis, though for clarity it is not removed in the plots in Figure 4.

3.0 Results and Projections

3.1 Vertical Land Motion

In our new solution (hereinafter referred to as "VLM10") we identify 68,193 high quality scatterers distributed throughout the Delta (Figure 5). This is roughly two times fewer targets than for our previous study from 1995-2000 with the ERS-2 satellite (hereinafter referred to as "VLM00") (Brooks et al., in press). The difference is predominantly because the ERS-2 scene covered substantially more area in the south and west of the Delta, which includes the extremely large number of scattering targets west of point P256 (Figure 5). In general, however, Envisat coherence within the Delta was reduced compared to ERS-2. As with our previous results, high-quality scattering targets are difficult to attain in the Delta interiors, and targets are limited to the levees.

As with our determination of VLM00 (Brooks et al., in press), the study uses the annual velocities of the three PBO stations and test a range of biases between -10 mm and +10 mm/yr to find the reference frame bias that minimizes the RMS-misfit between the CGPS and InSAR velocity fields for VLM10 (Figure 6). There is a clearly defined RMS minimum at +3 mm/yr, and so the InSAR results are adjusted accordingly (Figure 5). This reference frame bias is very close to the -2.9 mm/yr average annual vertical velocity at Plate Boundary Observatory GPS station P256, so this gives us further confidence to use it as a general reference point for the displacement rate map (Figure 5). It is important to note that in our previous study (Brooks et al. in press), we did not have as much confidence in our reference frame bias determination because there was no contemporaneously collected CGPS data.

3.2 Twenty-First Century Projection

As in Brooks et al. (in press), the spatial extent of the InSAR measurements allows us to make a projection of future levee subsidence and potential overtopping throughout much of the Delta given SLR scenarios and assuming that future subsidence rates follow the InSAR-measured ones. Although levee design standards in the Delta are variable (see Suddeth et al. 2010 for a review), for the purposes of a conservative and self-consistent analysis, all locations are assigned the PL 84-99 standard, wherein levees are designed to have ~0.5 m (1.5 ft.) freeboard above the 100-year flood stage (Betchart 2008). PL 84-99 is the federal target standard for two-thirds of Delta levees, although few meet this criteria: more conform to the Hazard Mitigation Plan (HMP) criteria of 1.0 ft. freeboard above the 100-year flood stage (Suddeth et al. 2010).

This study assumes that SLR in the Delta will not significantly differ from global estimates, and follows Vermeer and Rahmstorf's semi-empirical methodology relating sea level to global temperature change (Vermeer and Rahmstorf 2009) to project twenty-first century SLR for a variety of scenarios (Figure 10a). The Vermeer and Rahmstorf (2009) methodology ("SLR09") should be an improvement over the one from Rahmstorf (2007) ("SLR07") because it includes an additional term for instantaneous sea-level change as well as for longer-term changes. The result is a projection of significantly higher twenty-first century rates in comparison to SLR07: sea-level is predicted to be 1–1.9 m higher by 2100; whereas, SLR07 predicts a 0.5–1.4 m rise by 2100 (Figure 9).

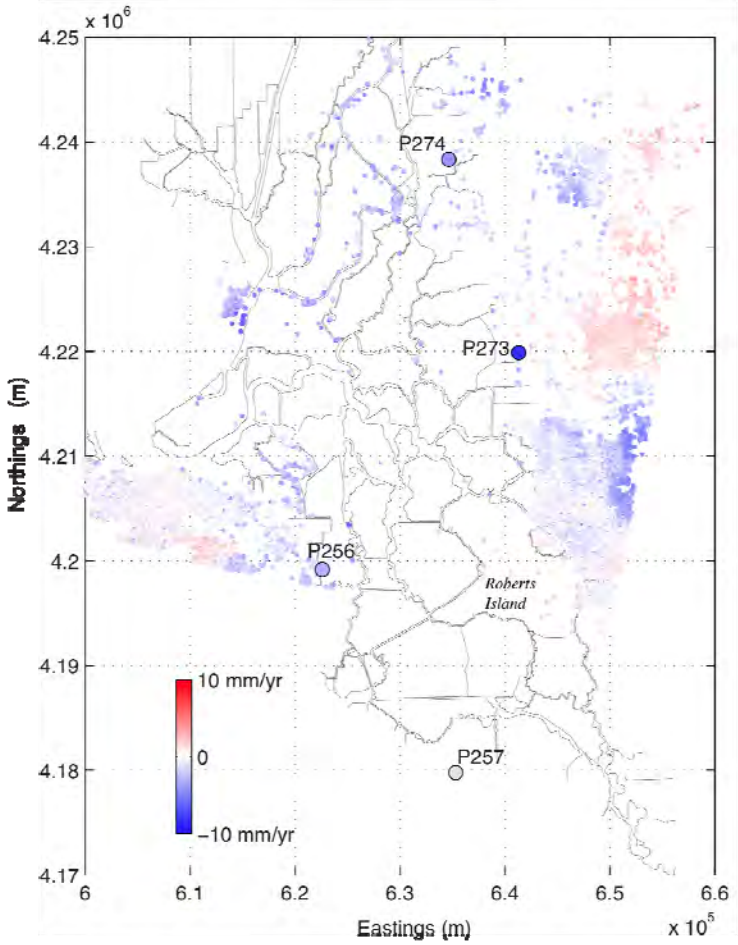

Figure 5. PSInSAR Annual Vertical Displacement Rates (Colored Small Circles) for All Scatterers from the 2006–2010 Envisat Data Set. Colored big circles are vertical displacement rate from Plate Boundary Observatory continuous GPS stations.

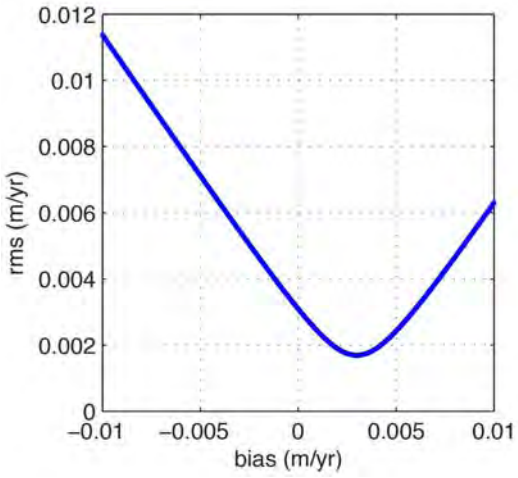

Figure 6. Plot of Reference Frame Bias vs. RMS Misfit Between CGPS Average Vertical Displacement Rate and Median InSAR Rate in 1km Radius Circle Around Each GPS Site

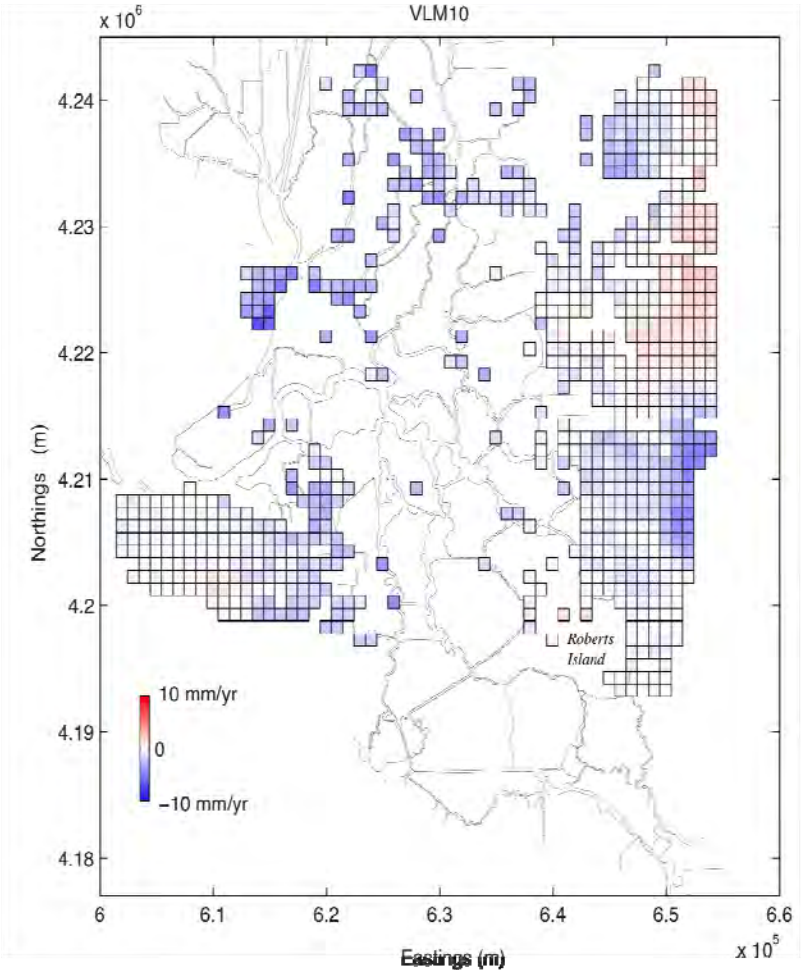

Figure 7. Colored Boxes, Median InSAR-derived Vertical Displacement Rate from All Scatterers in 1 x 1km Grid Cells

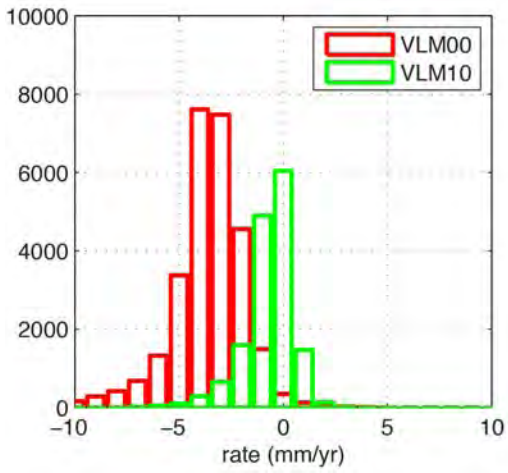

Figure 8. Histograms of Vertical Displacement Rates for All Scatters Within the Delta for the VLM00 and VML10 Solutions

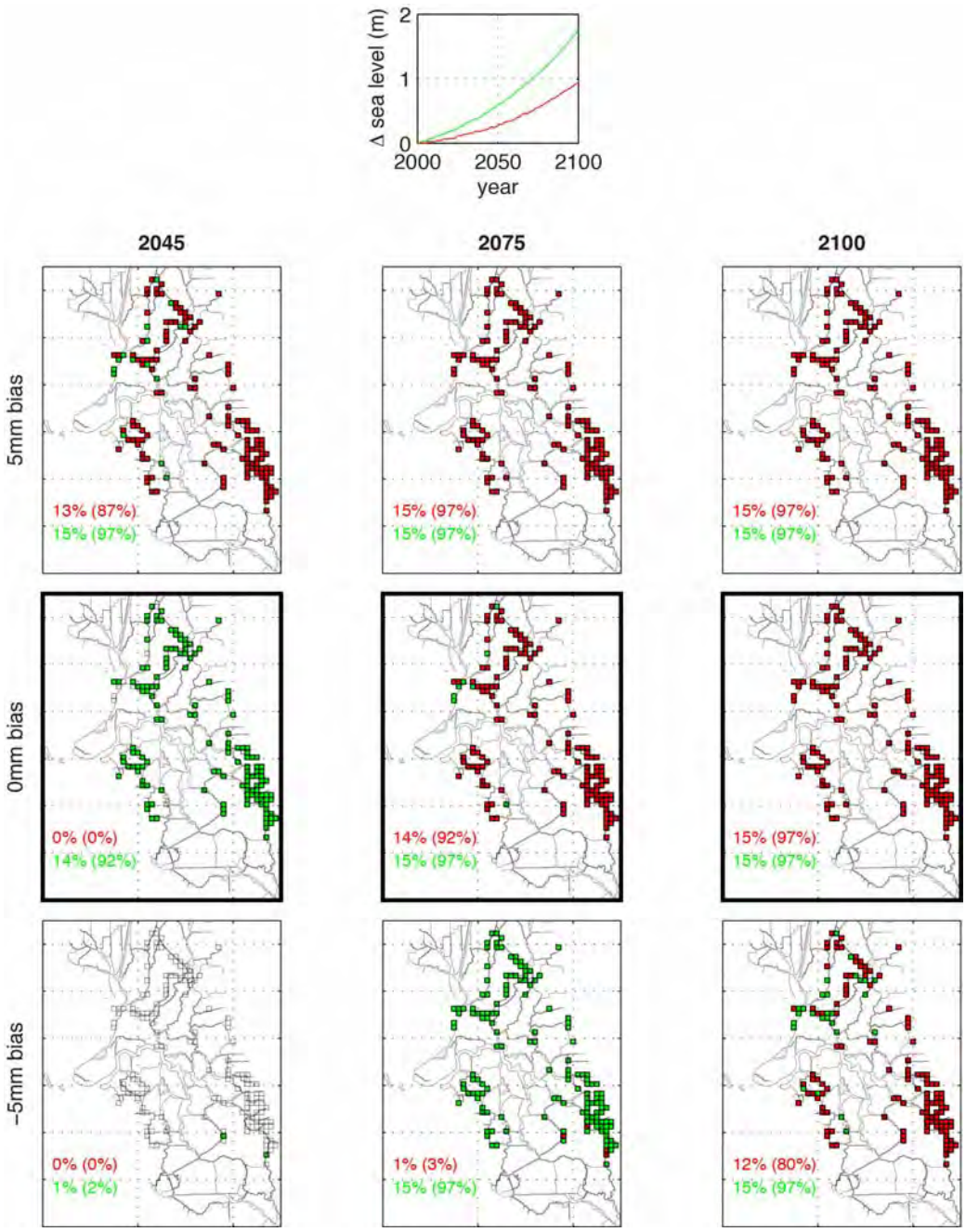

Figure 9. VLM10 Solution. (A) Projected sea-level rise in the Delta for low (red) and high (green) scenarios following Vermeer and Rahmstorf (2009). (B-J) Projected areas below 0.5 m of current elevation for 21st-century dates (columns), potential reference frame biases (rows), and sea-level rise scenarios (colored as in A). Colored text indicates percentage below threshold level: no parentheses, of all levees with InSAR measurements; parentheses, of all levees.

In addition to the lower and higher sea-level change projections, we also include possible reference frame biases in our matrix of overtopping projections (Figure 9). However, because of the contemporaneously collected CGPS data, we strongly prefer the "zero bias" projection (center row, Figure 9). The results suggest, under the minimum SLR scenario, by ~2050 the first levees will have subsided below design thresholds and by ~2075 more than 90 percent of the levees will have done so (assuming that the more sparse InSAR-derived rates are applicable Delta-wide). For the maximum SLR scenario, the dates change to ~2035 and ~2065, respectively. These results are not substantially different than our previous estimates based on VLM00 and SLR07. This agreement is, however, serendipitous: the higher subsidence rates are offset by the more accurate increased SLR rates. To more appropriately compare, if we use VLM00 with SLR09, then the dates when the first levees subside below threshold are ~2020 and 2025 (for high and low SLR curves); whereas, the dates when ~90 percent are below threshold are 2040 and 2060, respectively (Figure 10).

4.0 Discussion

Our results suggest that Delta levees will probably start to subside below design thresholds sometime between 2020 to 2035, and that from 2040 to 2075 more than 90 percent of them will have done so. Given that the earlier projected dates are from an earlier subsidence estimate (VLM00) and not the most recent one (VLM10), we suggest that the later rates are more likely. Due to a lack of a general time-varying physical model for the Delta subsidence mechanism, however, our only reasoning for this preference is based on assuming that future rates will follow modern ones. The InSAR-measured rates (VLM00 and VLM10) are close to an order of magnitude lower than measurements from island interiors at Sherman, Bacon, Mildred, or Lower Jones Islands (Deverel and Leighton 2010). As suggested in Brooks et al. (in press) the elevated subsidence rates of island interiors likely reflect elevated subsidence rates related to shallow peat compaction, and so for levee overtopping projections, they are less appropriate to use than the InSAR results.

It is unlikely that the difference between VLM00 and VLM10 can be explained in the context of the simple hydrological model delineated in Brooks et al. (in press). That study showed that, over the scale of five years, because the Delta land surface subsidence was contemporaneous with increasing aquifer and total river flow volume, the long-term subsidence process was not hydrologically controlled. During the 2006–2009 time period, total Delta flow decreased in comparison to the 1995–2000 period (Figure 11). If the Delta subsidence process were coupled with long-term Delta flow, we would expect that a decrease of water volume brought into the system by the Delta river flow would allow higher, rather than the lower subsidence rates observed in VLM10.

Previously, we suggested that compaction of the Delta Holocene sedimentary column underlying the shallow peat layers is the most likely a geologic process controlling the InSAR-derived subsidence rates; whereas, the local measurements (electrical tower pier level differences, for instance) most likely record shallow peat-related compaction. Sedimentary column compaction is a fundamental syndepositional and post-depositional diagenetic process that results in a reduction of sediment volume (Kaye and Barghoorn 1964; Allen 2000).

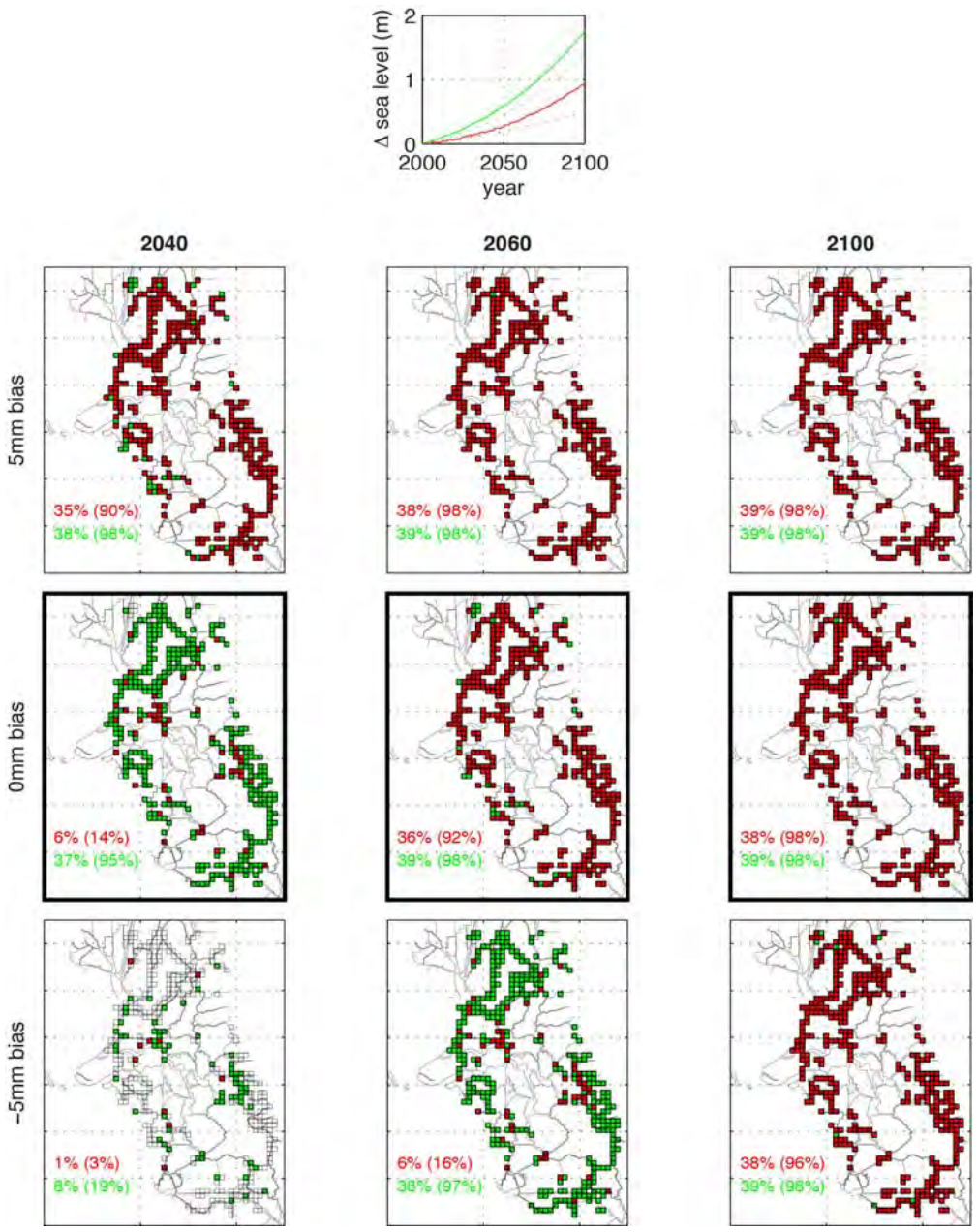

Figure 10. VLM00 Solution with the Vermeer and Rahmstorf (2009) Sea-level Rise Scenario. (A) Projected sea-level rise in the Delta for low (red), and high (green) scenarios following Vermeer and Rahmstorf (2009). (B-J) Projected areas below 0.5 m of current elevation for 21st century dates (columns), potential reference frame biases (rows), and sea-level rise scenarios (colored as in A). Colored text indicates percentage below threshold level: no parentheses, of all levees with InSAR measurements; parentheses, of all levees.

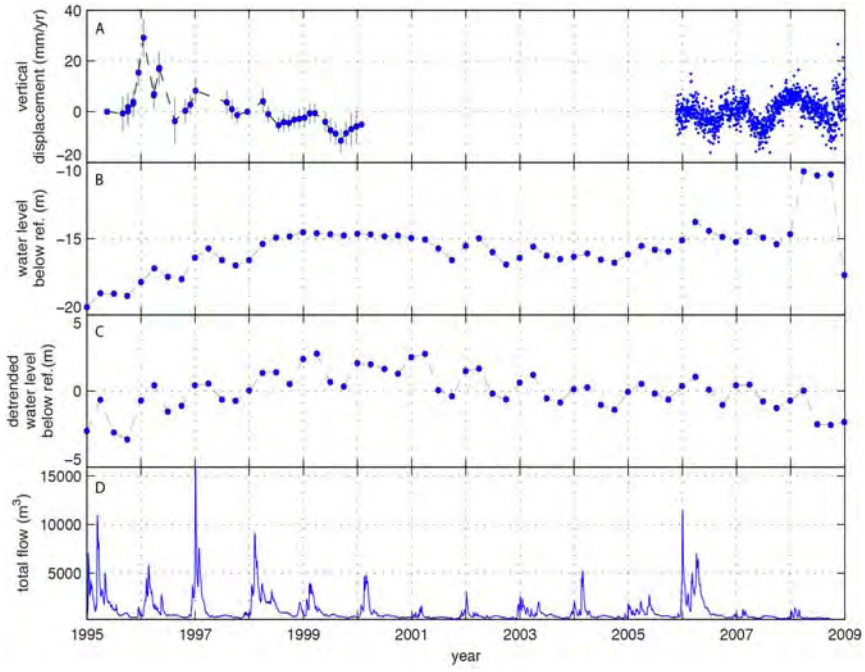

Source: Brooks et al. (in press)

Figure 11. (A) Blue Circles with 1 Sigma Error Bars, Median InSAR Time Series from VLM00 . Blue dots, time series from daily solutions for GPS station P257. The CGPS station, because it is on the Delta margin, does not record the average subsidence trend. (B) Blue Circles with 1sigma Error Bars, Median Time Series of Water Level Below Reference from Department of Water Resource Wells. (C) Total Flow from the Sum of Gauged Inflows from the Sacramento and San Joaquin River and the Streams on the East Side of the Delta, Department of Water Resources "DayFlow" Algorithm (http://www.iep.ca.gov/dayflow).

For example, Törnqvist et al. (2008) illustrated millennial-scale compaction rates of up to 5 mm/yr with local and/or decadal to centennial rates in excess of 10 mm/yr in the Mississippi and concluded that compaction of Holocene strata contributes significantly to the exceptionally high rates of relative sea-level rise there. Similarly, Horton and Shennan (2009) found compaction rates of up to 2.5 mm/yr along the east coast of England, with larger values associated with major estuaries. Nonetheless, the rate slowing from VLM00 to VLM10 is not one we would expect from a continuously compacting stratigraphic column.

An additional regional process that has heretofore been unexamined for the Delta is Glacial Isostatic Adjustment (GIA), the response of Earth's crust to the removal of the weight of the glacial ice masses (e.g., Peltier 2004). Since the submission of our first InSAR results, the PBO CGPS network has become mature enough so that its vertical velocity field may be examined. A map of annual vertical velocity for the PBO stations shows that much of the western United States exhibits subsidence at rates from 2–10 mm/yr (Figure 12). There is a clear GIA signal in the central and northeast portion of the North American continent due to removal of the Laurentide ice sheet (Argus and Peltier 2010; Sella et al. 2007) (Figure 12b); however, the

contribution of GIA to the western North American continent is less clear. For instance, the ICE4G model predicts essentially no subsidence west of the state of Utah; whereas, the ICE5G model predicts 1–2 mm/yr (Argus and Peltier 2010). Moreover, James et al. (2000) finds no evidence for GIA in geologic studies in the Pacific Northwest. They conclude that the viscosity values used by the GIA models are too high and therefore predict a spuriously long GIA time response. Thus, given the uncertainties in the GIA models it is difficult to unequivocally assess its contribution to Delta ground motion. Certainly GIA cannot explain any intra-Delta variation in subsidence rates, but we also cannot rule out the possibility that GIA may contribute a ~1–2 mm/yr subsidence signal.

The Roberts Island uplift signal further complicates the search for a simple, Delta-wide subsidence model. Given that the signal is in the opposite sense, and given that the spatial extent of this uplift signal is confined to a portion of the Delta, neither a Delta-wide process (Holocene section compaction) nor a regional (GIA) subsidence process can explain the observation. The localized nature of the signal suggests an aquifer-related explanation, such as poroelastic aquifer recharge (Schmidt and Burgmann 2003), and this would require detailed hydrological analysis that it outside the scope of this paper.

In summary, the current results have led us to conclude that Delta subsidence possibly has four different process components (shallow peat compaction, Delta holocene mineral soils and sedimentary section compaction, GIA, and aquifer poroelastic response) acting independently (Table 2). This demonstrates further the necessity of both a more sophisticated modeling approach that incorporates the synoptic InSAR monitoring capability. As with the evolution of global SLR scenarios, we envision an approach that can iteratively update future models based on new observations and thereby provide increasingly accurate overtopping projections that can be used by organizations for planning and cost-estimation purposes.

Figure 12. Vertical Displacement Rates from Continuous GPS Stations in North America. Inset, vertical rates from Sella et al. (2007). Main frame, vertical rates from the most-recent PBO solution (http://pboweb.unavco.org/**).**

Table 2: Delta Subsidence Processes

Process	Region	Rate
Shallow Peat Compaction	Island Interiors	- cms/yr
Holocene Mineral Soils/Sediment Compaction	Delta-Wide/Levees	- mms/yr
Glacial Isostatic Adjustment	Delta-Wide	- 1–2 mm/yr
Aquifer Poroelastic	Intra-Delta	+/- mms/yr

5.0 References

Altamimi, Z., X. Collilieux, J. Legrand, B. Garayt, and C. Boucher (2007) "ITRF2005: A new release of the International Terrestrial Reference Frame based on time series of station positions and Earth Orientation Parameters." *Journal of Geophysical Research*, 112(B9).

Argus, D. F., and W. R. Peltier (2010) "Constraining models of postglacial rebound using space geodesy: A detailed assessment of model ICE-5G (VM2) and its relatives." *Geophysical Journal International,* 181(2): 697–723.

Betchart, W. B. (2008) Delta Levees - Types, Uses, and Policy Options *Rep.*, http://deltavision.ca.gov/ConsultantReports/DV_Infrastructure_Draft_10-27-08.pdf.

Brooks, B. A., M. Merrifield, J. Foster, C. Werner, F. B. Gomez, M., and S. Gill (2007) "Space Geodetic Determination of Spatial Variability in Relative Sea-level Change, Los Angeles Basin." *Geophysical Research Letters*, *34*(L01611), doi:10.1029/2006GL028171.

Brooks, B. A., G. Bawden, D. Manjunath, C. Werner, N. Knowles, J. Foster, J. Dudas, and D. Cayan (in press) "Contemporaneous Subsidence and Levee Overtopping Vulnerability, Sacramento-San Joaquin Delta." California *San Francisco Estuary and Watershed Science*.

Burgmann, R., P. A. Rosen, and E. J. Fielding (2000) "Synthetic Aperture Radar interferometry to measure Earth's surface topography and it's deformation." *Ann. Rev. Earth Planet. Sci.*, 28: 169–209.

Church, J. A., and N. J. White (2006) "A 20th century acceleration in global sea-level rise." *Geophys. Res. Lett.*, *33*(L01602).

Coons, T., C. E. Soulard, and N. Knowles (2008) High-Resolution Digital Terrain Models of the Sacramento/San Joaquin Delta Region, California *Rep.*

Department of Water Resources (2009) Delta Risk Management Strategy.

Deverel, S. J., and S. Rojstaczer (1996) "Subsidence of agricultural lands in the Sacramento-San Joaquin Delta, California: Role of aqueous and gaseous carbon fluxes." *Water Resources Research*, *32*(8): 2359–2367.

Deverel, S. J., and D. A. Leighton (2010) "Historic, Recent, and Future Subsidence, Sacramento-San Joaquin Delta, California, USA." *San Francisco Estuary and Watershed Science*, *8*(2): 1–23.

Deverel, S. J., B. Wang, and S. Rojstaczer (1998) Subsidence of organic soils, Sacramento-San Joaquin Delta, in *Land subsidence case studies and current research. Proceedings of the Joseph Poland Subsidence Symposium. Sudbury (MA): Association of Engineering Geologists*, edited by J. W. Borchers, pp. 489–502, Star Publishing Company, Belmont, California.

Dixon, T. H., F. Amelung, A. Ferretti, F. Novali, F. Rocca, R. Dokka, G. Sella, S.-W. Kim, S. Wdowinski, and D. Whitman (2006) "Subsidence and flooding in New Orleans." *Nature*, 441: 587–588.

Ferretti, A., C. Prati, and F. Rocca (2001) "Permanent Scatterers in SAR Interferometry." *IIEEE Trans. Geosci. Remote Sensing*, *39*(1): 8–20.

Galloway, D. L., D. R. Jones, and S. E. Ingebritsen (1999) "Land Subsidence in the United States." *U.S. Geological Survey Circular 1182*.

Hooper, A., H. Zebker, P. Segall, and B. Kampes (2004) "A new method for measuring deformation on volcanoes and other natural terrains using InSAR persistent scatterers." *Geophys. Res. Lett.*, *31*, doi:10.1029/2004GL021737.

Kampes, B. (2006) *Radar Interferometry Persistent Scatterer Technique*, Springer, Dordrecht, Netherlands.

Lund, J., E. Hanak, W. Fleenor, R. Howitt, J. Mount, and P. Moyle (2007) *Envisioning futures for the Sacramento-San Joaquin Delta*, 285 pp., Public Policy Institute of California, San Francisco.

Lund, J., E. Hanak, W. Fleenor, W. A. Bennett, R. E. Howitt, J. F. Mount, and P. B. Moyle (2010) *Comparing Futures for the Sacramento-San Joaquin Delta*, 229 pp., University of California Press, Berkeley and Los Angeles, California.

Mount, J., and R. Twiss (2005) "Subsidence, sea-level rise, seismicity in the Sacramento-San Joaquin Delta." *San Francisco Estuary and Watershed Science*, *3*(1), Article 5.

Rojstaczer, S., and S. J. Deverel (1993), "Time dependence in atmospheric carbon inputs from drainage of organic soils." *Geophys. Res. Lett.*, 20: 1383–1386.

Rojstaczer, S., and S. J. Deverel (1995) "Land Subsidence in Drained Histosols and Highly Organic Mineral Soils of California," *Soil Sci Soc Am J*, 59(4): 1162–1167.

Rojstaczer, S., R. E. Hamon, S. J. Deverel, and C. Massey (1991) Evaluation of selected data to assess the causes of subsidence in the Sacramento-San Joaquin Delta, California *Rep.*, Sacramento, California.

Schmidt, D. A., and R. Burgmann (2003) "Time-dependent land uplift and subsidence in the Santa Clara valley, California, from a large interferometric synthetic aperture radar data set," *Journal of Geophysical Research, B, Solid Earth and Planets*, 108(B9), 2416.

Sella, G. F., S. Stein, T. H. Dixon, M. Craymer, T. S. James, S. Mazzotti, and R. K. Dokka (2007) "Observation of glacial isostatic adjustment in "stable" North America with GPS, *Geophysical Research Letters*, *34*(2).

Suddeth, R. J., J. F. Mount, and J. R. Lund (2010) "Levee Decisions and Sustainability for the Sacramento-San Joaquin Delta," *San Francisco Estuary and Watershed Science*, 8(2), 1–23.

Vermeer, M., and S. Rahmstorf (2009) "From the Cover: Global sea-level linked to global temperature." *Proceedings of the National Academy of Sciences*, *106*(51): 21527–21532.

Werner, C., U. Wegmüller, T. Strozzi, and A. Wiesmann (2003) Interferometric Point Target Analysis for Deformation Mapping, paper presented at IGARSS'03, Toulouse, France.

Woppelmann, G., C. Letetrel, A. Santamaria, M.-N. Bouin, X. Collilieux, Z. Altamimi, S. D. P. Williams, and B. M. Miguez (2009) "Rates of sea-level change over the past century in a geocentric reference frame." *Geophys. Res. Lett.*, *36*(L12607).

Glossary

CGPS	Continuous Global Positioning System
CR	Coast Range Mountains
DWR	California Department of Water Resources
GIA	Glacial Isostatic Adjustment
GPS	Global Positioning System
InSAR	Synthetic Aperture Radar Interferometry
ITRF	International Terrestrial Reference Frame
PBO	Plate Boundary Observatory
PSInSAR	Persistent Scatterer Interferometry
RMS	Root Mean Squared
SAC	Sacramento River Valley
SFB	San Francisco Bay
SJ	San Joaquin River Valley
SLR	Sea-Level Rise
SN	Sierra Nevada Mountains
VLM	Vertical Land Motion